Mathematical theory of molecular motors and a new approach for uncovering motor mechanism

H. Wang

Abstract: Molecular motors operate in an environment dominated by thermal fluctuations. A molecular motor may produce an active force at the reaction site to directly move the motor forward. Alternatively a molecular motor may generate a unidirectional motion by rectifying thermal fluctuations. In this case, the chemical reaction establishes free energy barriers to block the backward fluctuations. The effect of the chemical reaction on the motor motion can be represented by the motor potential profile (rectifying barrier and/or active driving force). Different motor mechanisms are characterised by different motor potential profiles. The mathematical theory and properties of molecular motors are discussed and a mathematical framework is developed for extracting the motor potential profile from measured time series of motor position. As an example, we discuss the binding zipper model for the F_1 ATPase, which was motivated mainly by the fact that the motor potential profile of the F_1 ATPase is nearly a constant slope.

1 Introduction

Protein motors play a central role in many cell functions. For example, myosin drives muscle contraction, kinesin drives intracellular vesicle transportation and moves chromosomes during mitosis, and the V-ATPases regulate intracellular acidity. Understanding the operating principles of protein motors is crucial to comprehending intracellular protein transport and cell motility. From the bioengineering point of view, understanding the operating principles of protein motors is crucial to incorporating protein motors into artificial systems, artificially controlling protein motors and manufacturing artificial motors.

Two key characters of molecular motors distinguish them from macroscopic motors; the motor motion is dominated by thermal fluctuations and the effect of inertia is negligible [1]. For a molecular motor, the instantaneous velocity fluctuations are several orders of magnitude larger than its average velocity. A unidirectional motion may be generated by allowing thermal fluctuations in the favoured direction while blocking those in the opposite direction. Such a motor is generally called a Brownian ratchet [2–6]. For a Brownian ratchet, there is no kinetic energy flow from the reaction site to the motor motion and the motor is moved directly by thermal fluctuations. Thus, a Brownian ratchet cannot operate without thermal fluctuations. It should be emphasised that the free energy for the unidirectional motion comes from the chemical reaction. Without the rectifying barriers established by the reaction, the forward and backward fluctuations are equally likely, and on average there is no unidirectional motion. Another way of generating a unidirectional motion is to produce an active force at the reaction site and use it to directly move the motor forward. Such a motor is generally called a power stroke motor [7, 8]. In a hypothetical situation, a power stroke motor could operate in the absence of thermal fluctuations if the chemical reaction and force production at the reaction site were not affected by the lack of thermal fluctuations (of course, in a realistic situation, the chemical reaction will not happen in the absence of thermal fluctuations). In [9], two representative models were considered for chemically driven transport; information ratchet and energy ratchet. The information ratchet in [9] corresponds to the Brownian ratchet in this article, while the energy ratchet in [9] has a large component of power stroke and a small component of Brownian ratchet.

The current experimental technologies permit measurement of forces and motions of a single protein motor to the precision of piconewtons and nanometers [10–14]. In the past, the measured time series of motor position were used to calculate the average velocity and the randomness parameter of the motor [10, 15]. The time series actually contain more information. We use a motor potential profile to represent the effect of the chemical reaction on the motor motion. For a Brownian ratchet, the potential profile is a sequence of vertical free energy drops acting as rectifying barriers when the motor tries to fluctuate backward. For a power stroke motor, the potential profile is a gradually decreasing function of the motor position. Brownian ratchet and power stroke motor are two extreme situations. The potential profile of a motor may have both vertical free energy drops and gradually decreasing slopes. The potential profile is the link between the chemical reaction and the motor motion. More important, it can be reconstructed from measured time series of motor position. Thus, the potential profile is a measurable quantity that provides insight into the physical mechanism of energy transduction.

Below, we will first discuss the effects of thermal fluctuations and inertia, and introduce the mathematical framework for modelling molecular motors. Then we will define the motor potential profile and describe an approach for reconstructing it from the measured time series of motor position. After that we will discuss the Stokes efficiency for motors working against viscous drag, and decompose the Stokes efficiency into two components; a 'chemical'

IEE Proceedings online no. 20031075

doi:10.1049/ip-nbt:20031075

Paper first received 17th June 2003 and in revised form 12th September 2003

The author is with the Department of Applied Mathematics and Statistics, University of California, Santa Cruz, CA 95064, USA

component measuring how efficiently the potential profile is generated in the chemical reaction and a 'mechanical' component measuring how efficiently the potential profile drives the motion. Finally, we will discuss what the potential profile tells about the motor mechanism. As an example, we will discuss the binding zipper model for the F_1 ATPase. The binding zipper model was mainly motivated by the assertion that the potential profile of the F_1 ATPase is nearly a constant slope.

2 Mathematical description and properties of molecular motors

The one-dimensional motion of an object in a fluid environment subject to a potential ϕ_S is described by the Langevin equation

$$m\frac{dv}{dt} = -\underbrace{\zeta v}_{\substack{\text{drag}\\ \text{force}}} - \underbrace{\phi_s'(x)}_{\substack{\text{force from}\\ \text{potential}}} + \underbrace{\sqrt{2k_BT\zeta}f(t)}_{\substack{\text{Brownian}\\ \text{force}}} \qquad (1)$$

where $v(t)$ is the velocity of the object, m the mass, ζ the drag coefficient, k_B the Boltzmann constant and T the absolute temperature [16].

2.1 Time scale of inertia and thermal excitations

In the absence of a potential, the object relaxes to thermal equilibrium with the environment. Both the average velocity and the average kinetic energy relax with a time scale of

$$t_0 = \frac{m}{\zeta}$$

$$\langle v(t)\rangle = \langle v(0)\rangle \exp\left(\frac{-t}{t_0}\right) \qquad (2)$$

$$\frac{1}{2}m\left\langle v(t)^2\right\rangle = \frac{1}{2}k_BT + \left(\frac{1}{2}m\left\langle v(0)^2\right\rangle - \frac{1}{2}k_BT\right)\exp\left(\frac{-2t}{t_0}\right) \qquad (3)$$

Equation (2) shows that the effect of initial velocity decays with a time scale of t_0. Thus, it is a matter of time scale when we look at the effect of inertia. If we are interested in the behaviour for time scales much larger than t_0, we can safely ignore the effect of inertia. For molecular motors, the time scale t_0 is very small. A 1 μm bead in water yields $t_0 \approx 56 \times 10^{-9} = 56$ ns. This is much smaller than the time scale of the motor reaction cycle.

Equation (3) shows that the thermal fluctuations typically change the kinetic energy of the object by an amount of k_BT in a time scale of t_0. The importance of thermal fluctuations is determined by comparing k_BT/t_0 with the rate of energy transduction. For molecular motors, k_BT/t_0 is much larger than the energy transduction rate. For example, a 1 μm bead in water yields $k_BT/t_0 \approx 1.8 \times 10^7$ k_BT/s while the energy consumption rate for a kinesin dimer is bounded by 2000 k_BT/s (at a hydrolysis rate of 100 ATP/s [17]). It should be noted that for a 1 μm bead in thermal equilibrium with the environment, the root-mean-square velocity is huge

$$\sqrt{\langle v^2\rangle} = \sqrt{\frac{k_BT}{m}} \approx 2.8 \times 10^3\ \mu\text{m/s}$$

In contrast, the maximum average velocity of a kinesin dimer is 1 μm/s [18]. In general, for molecular motors, the fluctuations in the instantaneous velocity are several orders of magnitude larger than the average velocity.

2.2 Stochastic evolution of the motor system (Langevin formulation)

Molecular motors operate in a fluid environment. Their size is generally of the order ~10 nm. The cargoes that molecular motors drive can be in the micron range [19]. The time scale of reaction cycles in molecular motors is 1 ms or longer; much larger than the time scale of inertia. As a result, the effect of inertia can be ignored for molecular motors. In each chemical state, the mechanical motion is described by a Langevin equation

$$\underbrace{\zeta\frac{dx}{dt}}_{\substack{\text{viscous}\\ \text{drag force}}} = \underbrace{-\phi_s'(x)}_{\substack{\text{motor}\\ \text{force}}} - \underbrace{F_{load}(x)}_{\substack{\text{load}\\ \text{force}}} + \underbrace{\sqrt{2k_BT\zeta}f(t)}_{\substack{\text{Brownian}\\ \text{force}}} \qquad (4)$$

where F_{Load} is an externally applied conservative force and ϕ_S is the periodic potential corresponding to the chemical state S of the motor system.

In our study, the motor system contains the motor, the cargo and (if applicable) the polymer track the motor is interacting with. In the experimental setup in [10], the kinesin motor system contains the kinesin dimer, the latex bead and the microtubule. The force clamp is an external system that exerts a conservative load force on the motor system. In the experimental setup in [13], the F_1 motor system contains the F_1 ATPase and the actin filament. These two experimental setups are schematically shown in Fig. 1. In our study, the chemical state of the motor system refers to the occupancy state of the reaction sites and the interaction state of the motor with the polymer track.

The phase space for the motor system is the product of a continuous variable $x(t)$ indicating the motor position, and

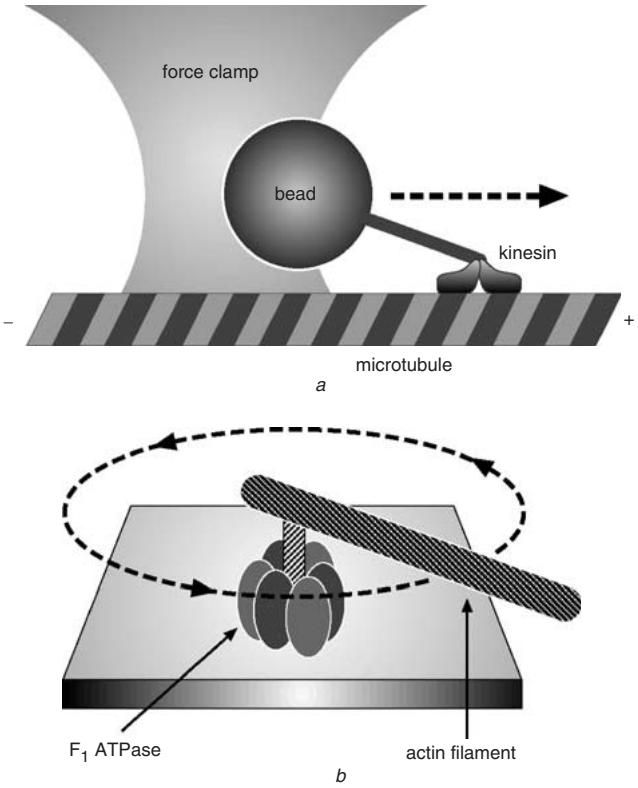

Fig. 1 *Experimental setups for measuring mechanical properties*
a Kinesin [10]
The kinesin motor moves along a microtubule, towing a large latex bead. A force clamp exerts a constant load force on the bead
b F_1 ATPase [13]
The bottom of the F_1 ATPase is attached to a coverslip. The rotating shaft drives a long actin filament

a discrete reaction coordinate $S(t)$ indicating the occupancy state of the motor system. We model the chemical transition (change of occupancy state) as a discrete Markov process. The stochastic evolution of occupancy state can be symbolically written as

$$\frac{d\boldsymbol{s}(t)}{dt} = \boldsymbol{K}(x)\cdot\boldsymbol{s}(t), \quad \boldsymbol{s}(t) = \{s_1, s_2, \ldots, s_N\} \tag{5}$$

Here $\{s_1, s_2, \ldots, s_N\}$ represents the set of all occupancy states of the motor system. $\boldsymbol{K}(x) = \{k_{ij}(x)\}$ is the matrix of transition rates: $k_{ij}(x)$ is the transition rate from state s_j to state s_i.

For ATPase motors, the ATP hydrolysis cycle at each catalytic site goes through four occupancy states [20–22]

$$\mathrm{CS} + \mathrm{ATP} \overset{\text{binding}}{\longleftrightarrow} \mathrm{CS}\cdot\mathrm{ATP} \overset{\text{hydrolysis}}{\longleftrightarrow} \mathrm{CS}\cdot\mathrm{ADP}\cdot\mathrm{P}_i$$
$$\overset{\mathrm{P}_i\text{release}}{\longleftrightarrow} \mathrm{CS}\cdot\mathrm{ADP} + \mathrm{P}_i \overset{\text{ADP release}}{\longleftrightarrow} \mathrm{CS} + \mathrm{ADP} + \mathrm{P}_i$$

The ATP hydrolysis cycle involves more than just the change of occupancy. For example, in the ATP binding process, an ATP in solution first diffuses to the catalytic site and is weakly bound (ATP docking). Then the ATP proceeds from weak binding to tight binding (the binding transition). During the binding transition, the bonds between the ATP and the catalytic site form progressively, and each bond formation drives a small conformational change of the catalytic site. A more accurate diagram for the ATP binding process is [8, 23]

$$\mathrm{CS} + ATP \overset{\text{ATP docking}}{\longleftrightarrow} \underbrace{\mathrm{CS}\cdot ATP}_{\text{APT weakly bound}}$$
$$\leftrightarrow \cdots \overset{\text{binding transition}}{\longleftrightarrow} \cdots \leftrightarrow \underbrace{\mathrm{CS}\bullet ATP}_{\text{APT tightly bound}}$$

here the size of dot represents the binding affinity of the ATP. In the mathematical formulation, only the change of occupancy (e.g. the ATP docking) is modelled by the Markov process (5). The part of the reaction that is directly coupled to the mechanical motion (e.g. the binding transition) is modelled as the motor driving force $-\phi_S'(x)$ in (4).

If the motor interacts with a polymer track, the occupancy state also reflects this interaction. For example, the interaction between a kinesin dimer and a microtubule has at least two states; one head attached or two heads attached. In the mathematical formulation, only the change of interaction state (e.g. docking and detaching of a kinesin head from the microtubule) is modelled by the Markov process (5). The change of interaction that is directly coupled to the mechanical motion (e.g. the transition from weak to strong binding of a kinesin head to the microtubule) is modelled as the motor driving force $-\phi_S'(x)$ in (4).

The stochastic evolution of the motor system (the mechanical motion and the chemical reaction) is described by (4) and (5).

2.3 Evolution of the probability density (Fokker–Planck formulation)

In experiments, only average quantities can be reliably observed or calculated. These average quantities include (but are not limited to) average velocity, reaction rate, effective diffusion coefficient, randomness parameter and the motor potential profile. In mathematical modelling, to compute average quantities of the motor system, we only need to follow the evolution of the probability density. Let $\rho_j(x, t)$ be the probability density of finding the motor system at position x and in occupancy state s_j at time t. The evolution of $\rho_j(x, t)$ is governed by a set of coupled Fokker–Planck equations which ensures the conservation of probability [24, 25]

$$\frac{\partial\rho_j}{\partial t} = \underbrace{\frac{1}{\zeta}\frac{\partial}{\partial x}\left(F_{Load}\rho_j + \phi_j'(x)\rho_j\right)}_{\substack{\text{effect of the load force}\\ \text{and the active motor force}}} + \underbrace{D\frac{\partial^2\rho_j}{\partial x^2}}_{\substack{\text{Brownian}\\ \text{motion}}} + \underbrace{\sum_{i=1}^{N} k_{ji}(x)\rho_i}_{\substack{\text{chemical}\\ \text{reactions}}} \tag{6}$$

where $D = k_B T/\zeta$ is the diffusion coefficient. Notice that, although (6) is linear in terms of ρ_j, it is nonlinear in terms of the vector $(\rho_j, F_{Load}, \phi_j(x), D, k_{ji}(x))$. Therefore, in general, the motor system does not respond linearly to the changes in the environment. In particular, the average velocity is generally not a linear function of the external load force. Equation (6) is the general mathematical framework for theoretical discussion of molecular motors [6, 26–31].

Figure 2 shows two hypothetical motor systems. The system shown in Fig. 2*a* is a Brownian ratchet. It is a simplified version of the two half-channel model for the bacterial flagellar motor [32, 33]. $\phi_1 \to \phi_2 \to \tilde{\phi}_1$ represents one proton translocation cycle. It is important to distinguish ϕ_1 and $\tilde{\phi}_1$ when discussing energetics. Transition ϕ_1 to ϕ_2 (② to ③) represents proton binding from the high concentration side. Transition ϕ_2 to $\tilde{\phi}_1$ (④ to ⑤) represents proton release to the low concentration side, which is very different from transition ϕ_2 to ϕ_1. The shaded regions indicate where the transitions can occur. Notice that the transition region of ϕ_1 to ϕ_2 does not overlap with that of ϕ_2 to $\tilde{\phi}_1$. This is necessary for preventing futile proton translocation not coupled to motor motion. In this motor system, the unidirectional motion is generated by rectifying thermal fluctuations. There is no active force to move the motor from ① to ②. However, a fluctuation to ② will be rectified if the system switches from ϕ_1 to ϕ_2 at ②.

The system shown in Fig. 2*b* is a power stroke motor. ①→②→③→④→⑤ represents one reaction cycle and one motor step. The potentials directly move the motor forward; ② to ③ is driven by potential ϕ_1 and ④ to ⑤ is driven by potential ϕ_2. However, the motion ② to ③ depends on transition ① to ②, and the motion ④ to ⑤ depends on transition ③ to ④. This motor system can be viewed as a much simplified model for the F_1 ATPase. The transition ① to ② represents the ATP docking, which initiates the power stroke generated by the ATP binding zipper [8, 23]. The transition ③ to ④ represents the ADP release, which is required for the completion of the power stroke. When the drag coefficient is large (e.g. the F_1 motor rotating a long actin), the motion is slow and the short pause waiting for ADP release is not detectable [12]. When the drag coefficient is small (e.g. the F_1 motor rotating a 40 nm gold bead), the pause waiting for ADP release is longer than the time scale of motion and can be resolved in experiments [34].

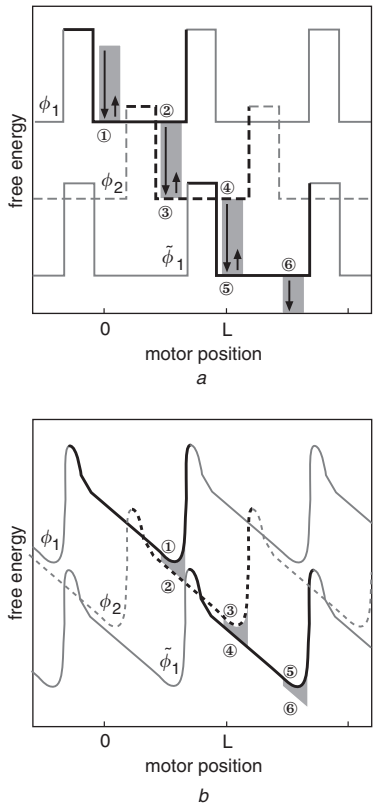

Fig. 2 *Two hypothetical motor systems*
In both panels, ①→②→③→④→⑤ represents one reaction cycle and one motor step. The vertical difference between ϕ_1 and $\tilde{\phi}_1$ is the free energy change of one cycle. The shaded regions indicate where the transitions between two potentials can occur
a Brownian ratchet. The potentials do not directly move the motor forward. Instead the unidirectional motion is generated by rectifying thermal fluctuations; the fluctuation ① to ② is rectified by the transition ② to ③
b Power stroke motor. The potentials directly move the motor forward. The motion ② to ③ is driven by potential ϕ_1. The transition ③ to ④ switches the system from the bottom of potential ϕ_1 to potential ϕ_2 so that the power stroke can continue

3 Motor potential profile

In single-molecule experiments, time series of motor position are recorded [10, 12]. In the past, only a value of average velocity and a value of randomness parameter were extracted from each time series [10, 15]. It is possible to extract more information from time series of motor position. At any given motor position, the total force driving the motor consists of two parts; the motor force from the chemical reaction ($-\phi_S'(x)$ in (4)) and the Brownian force from thermal fluctuations ($\sqrt{2k_BT\zeta}f(t)$ in (4)). Both forces are stochastic. The motor force is stochastic even if the motor position is known because the chemical state of motor system is stochastic. The recorded time series do not contain enough information about the chemical state. Therefore, it is unrealistic to extract all potential curves for N chemical states. However, if averaged over all chemical states weighted with corresponding probabilities at each motor position, the motor force depends only on the motor position. We call it the motor force profile and its integral is the motor potential profile. Although the motor potential profile does not contain all information about the potential curves and transition rates in (6), it does capture major features of the motor behaviour. At least it reveals more about the motor mechanism than just the average velocity. The biggest advantage of studying the potential profile is that it can be extracted from the measured time series of motor position.

Mathematically, the motor potential profile is defined as follows. At the steady state, if we sum over all N component equations of (6), we have

$$0 = \frac{1}{\zeta}\frac{\partial}{\partial x}(F_{Load}\rho + \psi'(x)\rho) + D\frac{\partial^2\rho}{\partial x^2} \tag{7}$$

where $\rho(x) = \sum_{j=1}^{N}\rho_j(x)$ is the probability density of finding the motor system at position x (regardless of chemical state). The motor potential profile $\psi(x)$ is defined as

$$\psi'(x) = \left(\sum_{j=1}^{N}\phi_j'(x)\rho_j(x)\right) \Big/ \left(\sum_{j=1}^{N}\rho_j(x)\right) \tag{8}$$

In [27], an effective potential for a two-state model was considered in a similar way. Equation (7) shows that at the steady state, the motor behaves as if it were driven by the potential $\psi(x)$. Thus, the motor potential profile represents the effect of the chemical reaction on the motor motion. Because $\psi'(x)$ is periodic, $\psi(x)$ can be written as

$$\psi(x) = \phi(x) + \frac{\Delta\psi}{L}x$$

where L is the motor step size and $\phi(x)$ is a periodic function with period L. $(-\Delta\psi) = \psi(0) - \psi(L)$ can be viewed as the potential energy per motor step available for driving the motor motion. How efficiently the potential energy $(-\Delta\psi)$ can be used to drive the motion depends on the shape of the potential profile $\psi(x)$. This will be discussed in the following Section.

Equation (8) does not provide us a direct way of calculating the potential profile $\psi(x)$ from experimental data. Instead, $\psi(x)$ can be reconstructed by solving the inverse problem of (7). In (7), the external load force F_{Load} is measured in experiments and $\rho(x)$ can be calculated from the measured time series of motor position. The probability density $\rho(x)$ calculated using a histogram analysis is not smooth. Even the exact $\rho(x)$ may have sharp jumps [3, 30]. Therefore, (7) and its inverse problem need special numerical treatments. We designed a robust numerical method that works even if $\rho(x)$ and $\psi(x)$ are discontinuous [35].

4 Stokes efficiency and its relation to motor potential profile

4.1 Thermodynamic efficiency

When a molecular motor works against a conservative load force exerted by an external system, the motor system consumes chemical energy and outputs potential energy to the external system. For example, when a kinesin dimer moves along a microtubule towing a bead against a force clamp [10], ATP hydrolysis free energy is consumed and the potential energy of the bead in the force clamp is increased (see Fig. 1*a*). In this case, the thermodynamic efficiency η_{TD} is defined as the energy conversion efficiency

$$\eta_{TD} = \frac{f_{Load}L}{-\Delta G} \tag{9}$$

where $-\Delta G$ is the free energy change of one reaction cycle (e.g. $-\Delta G \approx 20\ k_BT$ for the ATP hydrolysis cycle at physiological conditions [36]), f_{Load} the external load force (e.g. load exerted by the force clamp) and L the step size of

the motor (e.g. $L = 8$ nm for the kinesin dimer [18]). Here we define the motor step size as the displacement corresponding to one reaction cycle.

4.2 Stokes efficiency

When a molecular motor works against the viscous drag, the situation is completely different. First of all, the viscous drag is not a conservative force; it cannot be expressed as a function of motor position. The viscous drag opposes motion in any direction and it vanishes when the motor stops moving. In this situation, chemical energy is consumed but there is no energy output from the motor system. For example, in the experiments visualising the rotation of the F_1 ATPase, a long actin filament is attached to the rotating shaft [12, 13]. The F_1 motor works against the viscous drag on the filament. As the F_1 motor rotates, ATP hydrolysis free energy is consumed but there is no energy output from the motor system (recall that the F_1 motor system contains both the F_1 motor and the actin filament) (see Fig. 1*b*). The energy conversion efficiency is zero for the F_1 motor system. Nevertheless we want to measure how 'efficiently' the F_1 motor utilises the chemical free energy to drive the long actin filament through viscous fluid. When a motor works against the viscous drag, we define the Stokes efficiency (η_S) as [31, 37]

$$\eta_S = \frac{\zeta \langle V \rangle L}{-\Delta G} \tag{10}$$

where ζ is the drag coefficient and $\langle v \rangle$ the average velocity of the motor, and L the step size of the motor (e.g. $L = 120^\circ$ for the F_1 motor). It should be emphasised that every quantity in (10) is measurable in experiments. In (10), the denominator $(-\Delta G)$ is the free energy consumed per motor step. The numerator $\zeta \langle v \rangle L$ measures the mechanical performance of the motor. For fixed energy consumption, the larger the average velocity, the better the motor performance. However, the numerator does not have a clear thermodynamic meaning. In particular, the numerator is not the irreversible dissipation caused by the viscous friction. Therefore, it is not trivial to show that the Stokes efficiency defined in (10) is bounded by 100% [31]. Generally, for a molecular motor subject to both the viscous drag and the conservative load force, the Stokes efficiency is defined as $\eta_S = \zeta \langle v \rangle L/(-\Delta G + f_{Load} L)$.

4.3 Chemical component and mechanical component of the Stokes efficiency

The motor potential profile serves as the link between the chemical reaction and the motor motion. It is produced by the chemical reaction and used to drive the motion. Therefore, we can use it to decompose the overall Stokes efficiency into two components; a chemical component and a mechanical component.

As we discussed in the previous Section, $(-\Delta\psi) = \psi(0) - \psi(L)$ is the potential energy produced in one reaction cycle to drive the motion. The Stokes efficiency can be written as

$$\eta_S = \frac{\zeta \langle v \rangle L}{-\Delta G} = \underbrace{\left(\frac{-\Delta\psi}{-\Delta G}\right)}_{\substack{\text{chemical} \\ \text{component}}} \cdot \underbrace{\left(\frac{\zeta \langle v \rangle L}{-\Delta\psi}\right)}_{\substack{\text{mechanical} \\ \text{component}}} \tag{11}$$

The 'chemical' component $(-\Delta\psi)/(-\Delta G)$ measures how efficiently the chemical reaction generates the potential energy $(-\Delta\psi)$. The 'mechanical' component $(\zeta \langle v \rangle L)/(-\Delta\psi)$ measures how efficiently the potential energy $(-\Delta\psi)$ drives the motion. It can be shown that both of these two components are bounded by 100%. Therefore, if the Stokes efficiency is near 100%, then both components must be near 100%. The mechanical component of the Stokes efficiency is determined by the shape of the potential profile. From (7), one can show that

$$\frac{\zeta \langle v \rangle L}{-\Delta\psi} = \int_0^1 \exp\left(\frac{\Delta\psi}{k_B T} s\right) ds \Bigg/ \int_0^1 \left\{ \int_0^1 \exp \times \left(\frac{\phi(sL + \tilde{s}L) - \phi(\tilde{s}L)}{k_B T} \right) \right\} d\tilde{s} \cdot \exp\left(\frac{\Delta\psi}{k_B T} s\right) ds \tag{12}$$

If $\phi(x) = 0$ (i.e. the potential profile is a constant slope), then the mechanical component is 100%. Conversely, if the mechanical component is near 100%, then the potential profile must be close to a constant slope measured in units of $k_B T$. This has allowed us to deduce the potential profile for the F_1 motor directly from the high Stokes efficiency observed in experiments.

4.4 An example: the binding zipper model for the F_1 ATP synthase

The F_1 motor of ATP synthase provides a unique system to study the molecular mechanism whereby the chemical energy in the γ-phosphate bond of ATP is converted into a mechanical torque. Taking together the structural, biochemical and mechanical experimental results, we proposed the binding zipper model for the energy transduction mechanism of the F_1 ATP synthase [8, 23]. In the hydrolysis cycle, an ATP in solution first diffuses to the catalytic site and is weakly bound (ATP docking). Then the ATP proceeds from weak binding to tight binding (the binding transition). During the binding transition, the bonds between the ATP and the catalytic site form progressively, ATP binding affinity increases gradually, and each bond formation drives a small conformational change. In this way, the binding free energy is used efficiently to generate a nearly constant force during the multistep ATP binding transition. The role of hydrolysis is to weaken the binding and distribute it over the two products so that the products can be released and the cycle repeated. Conversely, in the synthesis cycle, the newly synthesised ATP is tightly bound to the catalytic site. The torque generated in the F_0 portion of the enzyme weakens the binding gradually from tight to weak until thermal fluctuations dislodge the ATP. The binding zipper model is in contrast to the models that assume that the elastic energy must be accumulated and then used all at once to release ATP [38]. In the binding zipper model, during both the hydrolysis and synthesis cycles, rotation is continuously coupled to the change of ATP binding affinity.

When we proposed the binding zipper model for the F_1 motor, one of the constraints was that the model should utilise nearly all free energy and produce a nearly constant motor torque. At that time, this constraint was put in, based on the analysis of a simple example, to match the experimental observation that the Stokes efficiency of the F_1 motor is near 100%. Now with the concept of motor potential profile and the decomposition of Stokes efficiency, we can justify this constraint. In (11), when the Stokes efficiency is near 100%, both the chemical component and the mechanical component must be near 100%, which implies that nearly all of the chemical energy is converted to the motor potential for driving the motion and that the potential profile is close to a constant slope.

The binding zipper model is not limited to the binding of ATP to the catalytic site. In walking motors (e.g. kinesins

and myosins), each head has two binding partners; nucleotide and the polymer track. Some or all of the force may be generated during the binding of head to track (e.g. kinesin head binding to microtubule, myosin head binding to actin). To repeat the force generation cycle, the binding of head to the track must be reset. The dissociation of myosin head from the actin is driven directly by the ATP binding zipper [39]. The dissociation of kinesin head from microtubule appears to be facilitated by the neck linker (another binding zipper) [40, 41], which, in turn, is driven by the ATP binding zipper.

5 Discussion

Molecular motors convert chemical energy to mechanical work while operating in an isothermal environment dominated by thermal fluctuations. In comparison with macroscopic motors, molecular motors have many peculiar characters:

(i) the time scale of inertia is much smaller than that of the reaction cycle

(ii) the rate of thermal excitations is much larger than the rate of free energy consumption

(iii) the instantaneous velocity fluctuations in a reaction cycle are several orders of magnitude larger than the average velocity

In contrast, for macroscopic motors, the velocity fluctuations in one reaction cycle are negligible (thinking about the velocity fluctuations of a motorcycle in a four-stroke cycle).

In this article, based on the mathematical framework for molecular motors, we defined and studied the motor potential profile, which is the link between the chemical reaction and the motor motion. The potential profile informs us about the motor mechanism. Most important, it can be reconstructed from the measured time series of motor position. Therefore, through the potential profile, theoretical studies can be related to experiments. Here the small size of molecular motors plays an interesting role. On one hand, the effort of deciphering the motor mechanism is, in many aspects, hindered by the small size. On the other hand, the small size eliminates the effect of inertia and makes it possible to uncover the motor force profile from time series. For macroscopic motors, the effect of inertia lasts over many cycles. Consequently, it is difficult to determine the force profile of a macroscopic motor from recorded motor positions. Just imagine trying to uncover the force profile of a single cylinder engine from recorded positions of a motorcycle.

Different motor mechanisms are characterised by different potential profiles. If the potential profile $\psi(x)$ is a constant slope, then the potential energy $(-\Delta\psi)$ is used uniformly to produce a constant force over the whole motor step. Such a motor is a power stroke motor. If the potential profile $\psi(x)$ is a flat step followed by a vertical drop, then the potential energy $(-\Delta\psi)$ does not produce an active driving force. Instead it produces a free energy barrier for rectifying thermal fluctuations. Such a motor is a Brownian ratchet. In general, the shape of the potential profile $\psi(x)$ tells us which fraction of a motor step is driven by a power stroke (active driving force) and which fraction is driven by a Brownian ratchet (barriers rectifying thermal fluctuations). The dependence of the average velocity (a scalar) on the external load force and reactant/product concentrations has already yielded valuable information about motor mechanism [42, 43]. The dependence of the potential profile (a function) on these factors will reveal more.

6 Acknowledgments

This work was supported by the US National Science Foundation.

7 References

1 Berg, H.C.: 'Random walks in biology', (Princeton University Press, Princeton, N.J., USA, 1993)
2 Peskin, C.S., Odell, G.M., and Oster, G.: 'Cellular motions and thermal fluctuations: the Brownian ratchet', *Biophys. J.*, 1993, **65**, pp. 316–324
3 Elston, T., Wang, H., and Oster, G.: 'Energy transduction in ATP synthase', *Nature*, 1998, **391**, pp. 510–514
4 Mogilner, A., and Oster, G.: 'The polymerization ratchet model explains the force-velocity relation for growing microtubules', *Eur. Biophys. J.*, 1999, **28**, pp. 235–242
5 Astumian, R.: 'Thermodynamics and kinetics of a Brownian motor', *Science*, 1997, **276**, pp. 917–922
6 Reimann, P.: 'Brownian motors: noisy transport far from equilibrium', *Phys. Rep.*, 2002, **361**, pp. 57–265
7 Wang, H., and Oster, G.: 'Energy transduction in the F1 motor of ATP synthase', *Nature*, 1998, **396**, pp. 279–282
8 Oster, G., and Wang, H.: 'Reverse engineering a protein: the mechanochemistry of ATP synthase', *Biochim. Biophys. Acta (Bioenerg.)*, 2000, **1458**, pp. 482–510
9 Astumian, R.D., and Derenyi, I.: 'Fluctuation driven transport and models of molecular motors and pumps', *Eur. Biophys. J.*, 1998, **27**, pp. 474–489
10 Visscher, K., Schnitzer, M., and Block, S.: 'Single kinesin molecules studied with a molecular force clamp', *Nature*, 1999, **400**, pp. 184–189
11 Hunt, A.J., Gittes, F., and Howard, J.: 'The force exerted by a single kinesin molecule against a viscous load', *Biophys. J.*, 1994, **67**, pp. 766–781
12 Yasuda, R., Noji, H., Kinosita, K., and Yoshida, M.: 'F_1-ATPase is a highly efficient molecular motor that rotates with discrete 120° steps', *Cell*, 1998, **93**, pp. 1117–1124
13 Noji, H., Yasuda, R., Yoshida, M., and Kinosita, K.: 'Direct observation of the rotation of F_1-ATPase', *Nature*, 1997, **386**, pp. 299–302
14 Sambongi, Y., Iko, Y., Tanabe, M., Omote, H., Iwamoto-Kihara, A., Ueda, I., Yanagida, T., Wada, Y., and Futai, M.: 'Mechanical rotation of the c subunit oligomer in ATP synthase (F_0F_1): direct observation', *Science*, 1999, **286**, pp. 1722–1724
15 Samuel, A., and Berg, H.: 'Fluctuation analysis of rotational speed of the bacterial flagellar motor', *Proc. Natl. Acad. Sci.*, 1995, **92**, pp. 3502–3506
16 Landau, L.D., Lifshitz, E.M., and Pitaevskii, L.P.: 'Statistical physics', 3rd Edn. (Pergamon Press, Oxford, New York, USA, 1980)
17 Hancock, W.O., and Howard, J.: 'Kinesin's processivity results from mechanical and chemical coordination between the ATP hydrolysis cycles of the two motor domains', *Proc. Natl. Acad. Sci. USA*, 1999, **96**, pp. 13147–13152
18 Schnitzer, M.J., and Block, S.M.: 'Kinesin hydrolyses one ATP per 8-nm step', *Nature*, 1997, **388**, pp. 386–390
19 Coppin, C., Pierce, D., Hsu, L., and Vale, R.: 'The load dependence of kinesin's mechanical cycle', *Proc. Natl. Acad. Sci. USA*, 1997, **94**, pp. 8539–8544
20 Abrahams, J., Leslie, A., Lutter, R., and Walker, J.: 'Structure at 2.8 Å resolution of F_1-ATPase from bovine heart mitochondria', *Nature*, 1994, **370**, pp. 621–628
21 Boyer, P.: 'The binding change mechanism for ATP synthase – some probabilities and possibilities', *Biochim. Biophys. Acta*, 1993, **1140**, pp. 215–250
22 Weber, J., and Senior, A.E.: 'Catalytic mechanism of F1-ATPase', *Biochim. Biophys. Acta*, 1997, **1319**, pp. 19–58
23 Oster, G., and Wang, H.: 'Rotary protein motors', *Trends Cell Biol.*, 2003, **13**, pp. 114–121
24 Risken, H.: 'The Fokker–Planck equation', 2nd Edn. (Springer–Verlag, New York, USA, 1989)
25 Gardiner, C.: 'Handbook of stochastic methods', 2nd Edn. (Springer–Verlag, New York, USA, 1985)
26 Ajdari, A., and Prost, J.: 'Mouvement induit par un potentiel périodique de basse symétrie: diélectrophorése pulsée', *C. R. Acad. Sci. Paris*, 1992, **315**, pp. 1635–1639
27 Prost, J., Chauwin, J., Peliti, L., and Ajdari, A.: 'Asymmetric pumping of particles', *Phys. Rev. Lett.*, 1994, **72**, pp. 2652–2655
28 Peskin, C.S., Ermentrout, G.B., and Oster, G.F.: in 'Mechanochemical coupling in ATPase motors', (Springer–Verlag, Les Houches, 1994)
29 Doering, C., Horsthemke, W., and Riordan, J.: 'Nonequilibrium fluctuation-induced transport', *Phys. Rev. Lett.*, 1994, **72**, pp. 2984–2987
30 Dimroth, P., Wang, H., Grabe, M., and Oster, G.: 'Energy transduction in the sodium F-ATPase of Propionigenium modestum', *Proc. Natl. Acad. Sci. USA*, 1999, **96**, pp. 4924–4929

31 Wang, H., and Oster, G.: 'The Stokes efficiency for molecular motors and its applications,' *Europhys. Lett.*, 2002, **57**, pp. 134–140
32 Meister, M., Caplan, S.R., and Berg, H.C.: 'Dynamics of a tightly coupled mechanism for flagellar rotation: bacterial motility, chemiosmotic coupling, protonmotive force', *Biophys. J.*, 1989, **55**, pp. 905–914
33 Berg, H., and Khan, S. *in* Sund, H. and Veeger, C. (Eds.) 'Mobility and recognition in cell biology' (de Gruyter, Berlin, Germany, 1983), pp. 485–497
34 Yasuda, R., Noji, H., Yoshida, M., Kinosita, K., and Itoh, H.: 'Resolution of distinct rotational substeps by submillisecond kinetic analysis of F1-ATPase', *Nature*, 2001, **410**, pp. 898–904
35 Wang, H., Peskin, C., and Elston, T.: 'A robust numerical algorithm for studying biomolecular transport process', *J. Theor. Biol.*, 2003, **221**, pp. 491–511
36 Stryer, L.: 'Biochemistry', 4th Edn. (W.H. Freeman, New York, USA, 1995)
37 Derenyi, I., Bier, M., and Astumian, D.: ' Generalized efficiency and its application to microscopic engines', *Phys. Rev. Lett.*, 1999, **83**, pp. 903–906
38 Kagawa, Y., and Hamamoto, T.: 'The energy transmission in ATP synthase: from the gamma-c rotor to the alpha-3-beta-3 oligomer fixed by OSCP-b stator via the beta-DELSEED sequence', *J. Bioenerg. Biomembr.*, 1996, **28**, pp. 421–431
39 Veigel, C., Coluccio, L., Jontes, J., Sparrow, J., Milligan, R., and Molloy, J.: 'The motor protein myosin-I produces its working stroke in two steps', *Nature*, 1999, **398**, pp. 530–533
40 Rice, S., Lin, A.W., Safer, D., Hart, C.L., Naber, N., Carragher, B.O., Cain, S.M., Pechatnikova, E., Wilson-Kubalek, E.M., Whittaker, M., Pate, E., Cooke, R., Taylor, E.W., Milligan, R.A., and Vale, R.D.: 'A structural change in the kinesin motor protein that drives motility', *Nature*, 1999, **402**, pp. 778–784
41 Mogilner, A., Fisher, A., and Baskin, R.: 'Structural changes in the neck linker of kinesin explain the load dependence of the motor's mechanical cycle', *J. Theor. Biol.*, 2001, **211**, pp. 143–157
42 Schnitzer, M., Visscher, K., and Block, S.: 'Force production by single kinesin motors', *Nature Cell Biol.*, 2000, **2**, pp. 718–723
43 Block, S., Asbury, C., Shaevitz, J., and Lang, M.: 'Probing the kinesin reaction cycle with a 2D optical force clamp', *Proc. Natl. Acad. Sci. USA*, 2003, **100**, pp. 2351–2356